Astron. Astrophys. 360, 439–446 (2000)

ASTRONOMY AND ASTROPHYSICS

NGC 4672: A new case of an early-type disk galaxy with an orthogonally decoupled core⋆,⋆⋆

M. Sarzi[1], **E.M. Corsini**[1], **A. Pizzella**[1], **J.C. Vega Beltrán**[2], **M. Cappellari**[3], **J.G. Funes S.J.**[3,4], **and F. Bertola**[3]

[1] Università di Padova, Osservatorio Astrofisico di Asiago, Dipartimento di Astronomia, Via dell'Osservatorio 8, 36012 Asiago, Italy
[2] Instituto Astrofísico de Canarias, Calle Via Lactea s/n, 38200 La Laguna, Spain
[3] Università di Padova, Dipartimento di Astronomia, Vicolo dell'Osservatorio 5, 35122 Padova, Italy
[4] University of Arizona, Vatican Observatory, Tucson, AZ 85721, USA

Received 15 February 2000 / Accepted 26 April 2000

Abstract. We report the case of the early-type disk galaxy NGC 4672 as a new example of a galaxy characterized by the orthogonal geometrical decoupling between bulge and disk. The morphological features of this galaxy are discussed as well as the velocity curves and velocity dispersion profiles of stars and ionized gas along both its major and minor axis. We conclude that NGC 4672 has structural (*i.e.* a bulge elongated perpendicularly to the disk) and kinematical (*i.e.* a stellar core rotating perpendicularly to the disk) properties similar to those of the Sa NGC 4698. The presence of the isolated core suggests that the disk component is the end result of the acquisition of external material in polar orbits around a pre-existing oblate spheroid as in the case of the ring component of AM 2020-504, the prototype of polar ring ellipticals.

Key words: galaxies: individual: NGC 4672 – galaxies: kinematics and dynamics – galaxies: spiral – galaxies: formation – galaxies: structure

1. Introduction

Most of the kinematically decoupled structures observed in galaxies have been considered to have an external origin, and to represent the end result of the acquisition of material coming from outside the boundaries of an already formed galaxy via infall, accretion or merging. The angular momenta of the acquired and pre-existing material are generally misaligned with respect to each other. In fact the angular momentum of the acquired material depends on the impact parameters of the capture process and on the geometry of the potential of the host galaxy. This is the case of the elliptical galaxies with a dust lane along their minor axis (see Bertola 1987 for a review) and of the polar-ring galaxies (see the photographic atlas of Whitmore et al. 1990), where the acquired gas (and its associated stars) is rotating around an axis orthogonal to the minor axis of the main stellar body. Moreover this is also the case of the Sa galaxy NGC 4698, where the presence of an orthogonal decoupling between bulge and disk has been recently discussed by Bertola et al. (1999).

The mass of the orthogonally rotating material is negligible ($M_{\rm gas} \lesssim 10^9$ M$_\odot$) with respect to the total dynamical mass of the host galaxy in the minor-axis dust-lane elliptical galaxies (Sage & Galletta 1993). The mass of the acquired gas ($M_{\rm gas} \approx 10^{10}$ M$_\odot$) is comparable or even greater than the mass of the pre-existing galaxy in the polar-ring galaxies, like the elliptical AM 2020-504 (Arnaboldi et al. 1993a), the S0 NGC 4650A (Sackett et al. 1994) and the spiral NGC 660 (van Driel et al. 1995). In NGC 4650A, the polar structure is massive enough to lead to the formation of a spiral pattern, as pointed out by Arnaboldi et al. (1997). This is a strong indication that in this object the acquired material settled onto a disk rather than forming a ring. Besides, there is a number of similarities between the global properties (e.g., total luminosity, integral colors, gas-to-dust ratio and star formation rate) of the polar-rings around S0's, and spirals and the properties of the disks of late-type spiral galaxies (see Reshetnikov & Sotnikova 1997 and references therein).

The case of the Sa galaxy NGC 4698 (Bertola et al. 1999) could represent the first example of an orthogonal acquisition involving an even larger amount of external material, which produced an intrinsic change of the galaxy morphology. In fact the geometric and kinematical orthogonal decoupling between the bulge and disk of this early-type spiral galaxy has been interpreted as the end product of the accretion of material which built up the disk component around a previously formed bare spheroid.

In the framework of massive acquisition processes, we present NGC 4672 as a new case of a disk galaxy characterized by a geometric and kinematical orthogonal decoupling between its bulge and disk. This paper is organized as it follows. In Sect. 2 we present our spectroscopic observations of NGC 4672. The morphology of this object and its classification are discussed in Sect. 3. The kinematical results for both the gaseous and the

Send offprint requests to: M. Sarzi (sarzi@pd.astro.it)

⋆ Based on observations carried out at ESO, La Silla (Chile).

⋆⋆ Tables 3 to 6 are only available in electronic form at the CDS via anonymous ftp to cdsarc.u-strasbg.fr (130.79.128.5) or via http://cdsweb.u-strasbg.fr/Abstract.html.

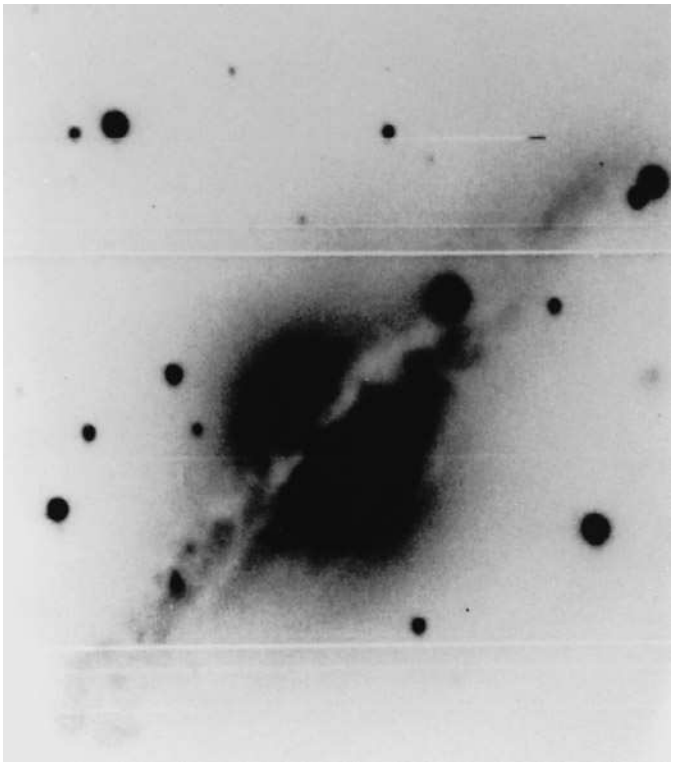

Fig. 1. NGC 4672 as it appears in Fig. 3i of the Polar-Ring Galaxy Catalog by Whitmore et al. (1990). The orientation of the image is north to right and east bottom.

stellar components are described in Sect. 4 and we move towards our conclusions in Sect. 5.

2. Observations and data reduction

The spectroscopic observations of NGC 4672 were carried out at the European Southern Observatory in La Silla during three different runs. We observed the galaxy at the Danish 1.54-m telescope on July 12, 1998 and at the ESO 1.52-m telescope on August 6, 1998 and on June 9-10, 1999 respectively.

The Danish 1.54-m telescope was equipped with the Danish Faint Object Spectrograph and Camera (DFOSC). We used the grism No. 7 with 600 grooves mm^{-1} and the Loral/Lesser C1W7 CCD, which has 2052×2052 pixels of $15 \times 15\,\mu\mathrm{m}^2$. We took six separate spectra of 30 minutes each along the minor axis of the galaxy ($\mathrm{P.A.} = 134°$) for a total exposure time of 3 hours. To position the slit on the galaxy center an acquisition image of 300 s was obtained in the R band using the ESO filter No. 452.

The Cassegrain Boller & Chivens spectrograph was mounted at the ESO 1.52-m telescope in combination with the grating No. 33 with 1200 grooves mm^{-1} and the Loral/Lesser CCD No. 39 with 2048×2048 pixels of $15 \times 15\,\mu\mathrm{m}^2$. We obtained a single 60-minutes spectrum and 4 separate spectra of 60 minutes along the galaxy major axis ($\mathrm{P.A.} = 46°$) in August 1998 and June 1999, respectively.

Every night a number of spectra of late-G and early-K giant stars were obtained to be used as template in measuring the stellar kinematics. Comparison spectra were taken before every object exposure. Further details of the instrumental set-up in the three observing runs are given in Table 1.

Using standard ESO-MIDAS[1] routines all the spectra were bias subtracted, flatfield corrected, cleaned from cosmic rays and calibrated. The spectra taken along the same axis in the same run were co-added using the center of the stellar continuum as reference. The contribution of the sky was determined from the edges of the resulting spectra and then subtracted.

The stellar kinematics was measured from the absorption lines present in the spectra using the Fourier Correlation Quotient Method (Bender 1990) as applied by Bertola et al. (1996). The values obtained for the stellar kinematics along the major and minor axis are reported in Tables 3 and 4, respectively. The ionized-gas kinematics was measured from the Hα and [N II] $\lambda 6583.41$ emission lines by means of the MIDAS package ALICE as done by Corsini et al. (1999). The gas velocity and velocity dispersion are the mean values obtained from the two emission lines. No error is given when only one velocity or velocity dispersion measurement is available. The kinematical data derived for the gaseous component along the major and minor axis are given in Tables 5 and 6, respectively.

The $R-$band acquisition image (Fig. 2) was bias subtracted and flatfield corrected. No attempt was made to perform an absolute calibration since the image was obtained under non-photometric condition.

3. The morphology of NGC 4672

NGC 4672 (ESO 322-G73) is a highly-inclined early-type disk galaxy classified as Sa(s) pec sp by de Vaucouleurs et al. (1991). An overview of the properties of NGC 4672 is given in Table 2.

The galaxy is characterized by an intricate dust pattern made of patches rather than lanes, which pervade the disk and cross the galaxy near the center of the bulge (Fig. 1). NGC 4672 is a dust-rich system as one can also infer by a comparison of its dust-to-blue luminosity ratio with the mean values found by Bregman et al. (1992) for the early-type disk galaxies studied by Roberts et al. (1991). The dust pattern is so relevant in determining the shape of NGC 4672 that Arp & Madore (1987) included it (with the name of AM 1243-412) in the section of the Catalogue of Southern Peculiar Galaxies devoted to the galaxies with prominent or unusual dust absorption. Corwin et al. (1985) pointed out a resemblance between the overall structure of NGC 4672 and that of NGC 5128 in their Southern Galaxy Catalogue. In spite of this similarity with a dust-lane elliptical they classified NGC 4672 a S0/a: pec sp galaxy since they recognized in the disk the presence of spiral arms. Recently, NGC 4672 has been included by de Grijs (1998) in a large sample of edge-on disk galaxies which have been observed in different optical and near-infrared passbands to study the global properties of galactic disks.

[1] MIDAS is developed and maintained by the European Southern Observatory

Table 1. Instrumental set-up of spectroscopic observations

Parameter	P.A. $= 134^\circ$	P.A. $= 46^\circ$	
Date	Jul 12, 1998	Aug 06, 1998	Jun 09-10, 1999
Instrument	Danish 1.54-m+DFOSC	ESO 1.52-m+B&C	
Scale	$0\farcs39$ pixel^{-1}	$0\farcs82$ pixel^{-1}	
Reciprocal dispersion	1.47Å pixel^{-1}	0.98Å pixel^{-1}	
Slit width	$1\farcs5$	$2\farcs4$	$2\farcs2$
Wavelength range	3847 – 6850 Å	4858 – 6872 Å	4813 – 6829 Å
Comparison-lines FWHM	5.58 ± 0.02 Å	2.77 ± 0.08 Å	2.86 ± 0.04
Instrumental σ at Hα	108 km s^{-1}	54 km s^{-1}	55 km s^{-1}
Exposure time	6×30 min	1×60 min	4×60 min
Seeing FWHM	$1\farcs8$ – $2\farcs2$	$1\farcs5$ – $2\farcs0$	$1\farcs5$ – $2\farcs5$

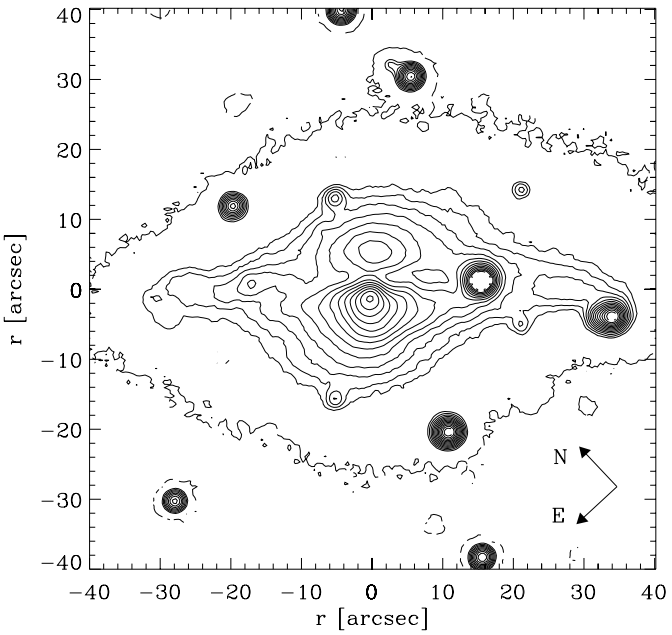

Fig. 2. $R-$band isophotes of NGC 4672 (boxcar smoothed over 3×3 pixels). The inner isophotes are given in steps of 0.25 (uncalibrated) mag between -3.5 and -0.5 mag (see Fig. 3), while the outermost isophote corresponds to a level of 1.0 mag.

Like in the case of NGC 4698 (Bertola et al. 1999), the bulge of NGC 4672 appears elongated in an orthogonal way with respect to the disk at a simple visual inspection of galaxy images (Fig. 1). This remarkable feature is confirmed by the shape of the inner ($|r| \lesssim 10''$) $R-$band isophotes, as shown in the isophotal map of NGC 4672 in Fig. 2.

For this peculiarity NGC 4672 has been included by Whitmore et al. (1990) in the Polar-Ring Galaxy Catalog as a possible candidate polar-ring galaxy (PRC C-42). They stated that even if long exposures show a fairly normal Sa galaxy, shorter exposures reveal that the bulge component of the galaxy is slightly elongated in a direction perpendicular to the disk. They considered this feature as a signature of the structure of a polar-ring galaxy, since the observed bulge and disk components of NGC 4672 could be interpreted respectively as an almost face-on disk and a nearly edge-on ring due to the orientation of the galaxy.

Table 2. Optical and radio properties of NGC 4672

parameter	value
Name	NGC 4672
Morphological type	.S.0∗P/ [a];.SAS1P/ [b]
Heliocentric systemic velocity [c]	3275 ± 20 km s^{-1}
Distance [c]	39.9 Mpc
Disk position angle [c]	46°
Apparent isophotal diameters [b]	$122\farcs5 \times 33\farcs7$
Inclination [c]	75°
Apparent B magnitude [d]	13.37 mag
Apparent corrected B magnitude [b]	12.96 mag
Absolute corrected B magnitude [c]	-20.04 mag
Total B luminosity L_B^0	$1.61 \cdot 10^{10}$ L$_{B,\odot}$
H I linewidth at 20% of the peak [e]	403 km s^{-1}
H I linewidth at 50% of the peak [e]	356 km s^{-1}
Mass of neutral hydrogen $M_{\rm HI}$ [f]	$2.88 \cdot 10^9$ M$_\odot$
$M_{\rm HI}/L_B^0$	0.18
Mass of cool dust $M_{\rm d}$ [g]	$4.17 \cdot 10^6$ M$_\odot$
$M_{\rm d}/L_B^0$	$2.59 \cdot 10^{-4}$

[a] from Corwin et al. (1985).
[b] from de Vaucouleurs et al. (1991). The apparent isophotal diameters are measured at a surface brightness level of $\mu_B = 25$ mag arcsec^{-2}.
[c] from this paper. The distance is derived as V_0/H_0 with V_0 the velocity relative to the centroid of the Local Group obtained from the heliocentric systemic velocity as in Sandage & Tammann (1981) and $H_0 = 75$ km s^{-1} Mpc^{-1}. The inclination i is derived as $\cos^2 i = (q^2 - q_0^2)/(1 - q_0^2)$, where the observed axial ratio corresponds to $q = 0.28$ (de Vaucouleurs et al. 1991) and an intrinsic flattening of $q_0 = 0.11$ has been assumed following Guthrie (1992).
[d] from de Grijs (1998).
[e] from Aaronson et al. (1989).
[f] from Richter et al. (1994) for the adopted distance.
[g] derived following Young et al. (1989) from the IRAS flux densities of NGC 4672 at 60 and 100 μm (Moshir et al. 1990).

However there is a number of reasons to reject the polar-ring classification and to consider the edge-on component of NGC 4672 a disk rather than a polar ring, and the face-on component a bulge rather than a low-inclined disk:

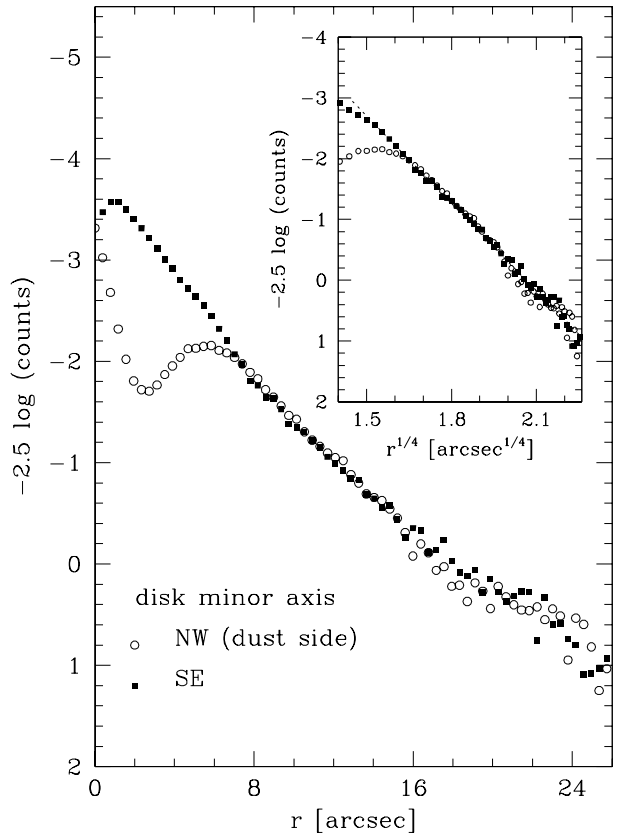

Fig. 3. Uncalibrated luminosity profile of NGC 4672 extracted along the major axis of the bulge component (*i.e.*, the galaxy minor axis at $\mathrm{P.A.} = 134°$). *Filled squares* and *open circles* represent the data obtained along the SE and the NW (dust affected) sides, respectively. The folding has been performed to obtain the best match of the luminosity profile on the two sides in the outer, dust-free region. In the inset the data are plotted adopting a $r^{1/4}$-radial scale and the *dashed-line* represents the best-fitting $r^{1/4}$ profile to the SE side data ($r_e = 9''$).

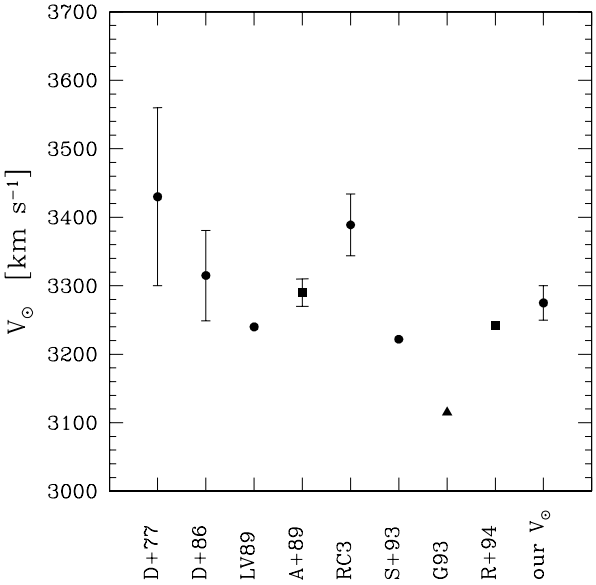

Fig. 4. Heliocentric systemic velocity of NGC 4672 derived from optical (*circles*), radio (*squares*) and optical and radio (*triangles*) measurements. D+77 = Dawe et al. (1977), D+86 = Dickens et al. (1986), LV89 = Lauberts & Valentijn (1989), A+89 = Aaronson et al. (1989), RC3 = de Vaucouleurs (1991), S+93 = Schommer et al. (1993), G93 = Garcia (1993), R+94 = Richter et al. (1994), our $V_\odot$ = this paper.

(i) From the uncalibrated $R-$band acquisition image we extracted the luminosity profile at $\mathrm{P.A.} = 134°$ along the major axis of the almost face-on component (*i.e.*, along the minor axis of the edge-on component). It turns out that this profile follows an $r^{1/4}$ law with an effective radius $r_e = 9''$ (Fig. 3). This indicates that we are looking at a stellar spheroid (*i.e.*, the bulge of an early-type disk galaxy or an elliptical galaxy) rather than a face-on disk.

(ii) The edge-on component contributes a large fraction of light to the total luminosity of the galaxy. In fact the disk-to-total luminosity ratio we derived from de Grijs (1998) is $D/T = 0.75$ in the $B-$band, and $D/T = 0.68$ in the $I-$band. The $B-$band D/T is a typical value for an intermediate-type spiral galaxy (Kent 1985; Simien & de Vaucouleurs 1986).

(iii) The ionized-gas rotation curve measured along the major axis of the edge-on component ($\mathrm{P.A.} = 46°$) exhibits the differential rotation (Fig. 5) typical of a disk component. The absence of the characteristic linear rise of the gas rotation velocity due to the so-called 'rim of the wheel' effect (*e.g.*, Vega Beltrán et al. 1997) is an indication that we are not facing an edge-on ring.

Summarizing, NGC 4672 edge-on component can not be a ring-like structure rotating around a low-inclined disk galaxy. Therefore the possibility that NGC 4672 could be a polar-ring galaxy dressed up as a spiral is ruled out. As a consequence, we assume as major-axis position angle of NGC 4672 that of the disk component ($\mathrm{P.A.} = 46°$) instead of the value of $\mathrm{P.A.} = 134°$ given by de Vaucouleurs et al. (1991) and corresponding to the apparent major axis of the bulge.

NGC 4672 was observed in the 21-cm neutral hydrogen line by Aaronson et al. (1989) and by Richter et al. (1994). The large H I linewidth suggests that most of this gas is associated with the edge-on disk.

4. The kinematics of NGC 4672

4.1. Heliocentric systemic velocity

We derived the heliocentric systemic velocity of NGC 4672 $V_\odot = 3275 \pm 20\,\mathrm{km\ s^{-1}}$ by fitting the major-axis rotation curves with a suitable odd function. In Fig. 4 we compare our heliocentric systemic velocity with previous determinations based on optical and radio measurements. It is in agreement within the 3σ error with the values given by Dawe et al. (1977, $V_\odot = 3430 \pm 130$ km s^{-1}), Dickens et al. (1986, $V_\odot = 3315 \pm 66$ km s^{-1}), Lauberts & Valentijn (1989, $V_\odot = 3240$ km s^{-1}), Aaronson et al. (1989, $V_\odot = 3290 \pm 20\,\mathrm{km\ s^{-1}}$), de Vaucouleurs et al. (1991, $V_\odot = 3389 \pm 45\,\mathrm{km\ s^{-1}}$), Schommer et al. (1993, $V_\odot = 3222$ km s^{-1}), Richter et al. (1994, $V_\odot = 3242$ km s^{-1}). Only the

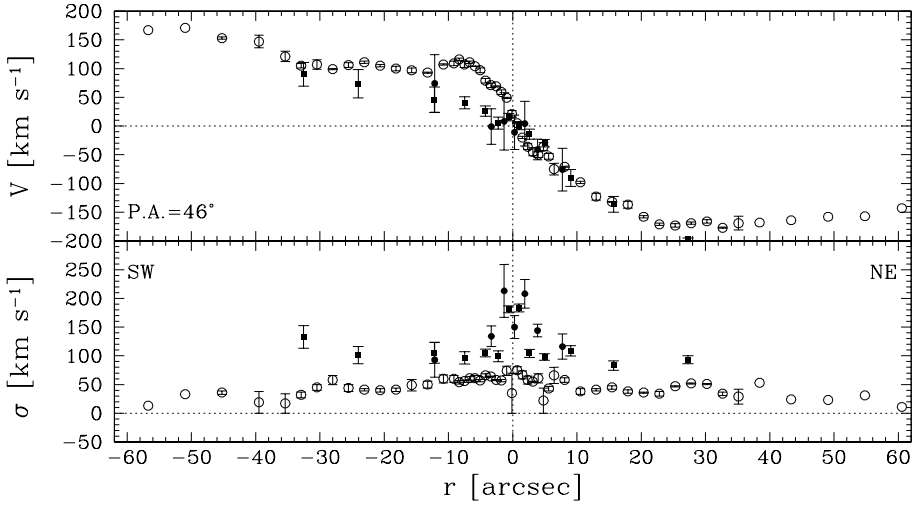

Fig. 5. The stellar (*filled symbols*) and ionized-gas (*open circles*) kinematics measured along the disk major axis (*i.e.*, the bulge minor axis at P.A. $= 46^{\circ}$) of NGC 4672. The systemic velocity is $V_{\odot} = 3275 \pm 20$ km s^{-1}. All rotation velocities are plotted as observed without applying any inclination correction. The *filled circles* and the *filled squares* represent data obtained in August 1998 and July 1999, respectively.

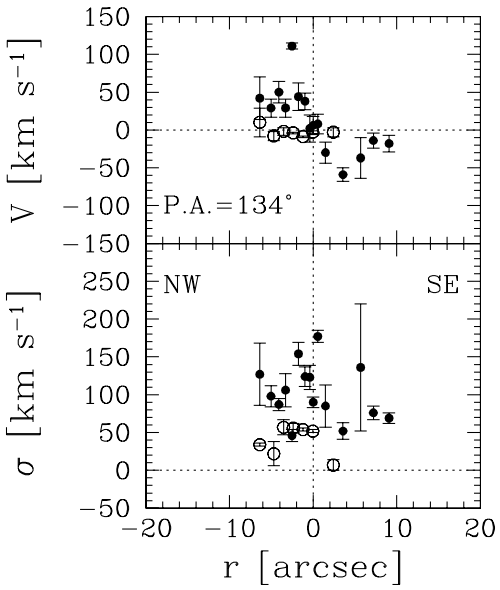

Fig. 6. The stellar (*filled circles*) and ionized-gas (*open circles*) kinematics measured along the disk minor axis (*i.e.*, the bulge major axis at P.A. $= 134^{\circ}$) of NGC 4672.

systemic velocity given by Garcia (1993, $V_{\odot} = 3115$ km s^{-1}) does not fall in this range.

The position-velocity curves and velocity dispersion profiles we measured for the stellar and gaseous components along the major and minor axis of NGC 4672 are presented in Fig. 5 and Fig. 6, respectively.

At each radius the plotted velocities V of ionized gas and stars are the observed ones after subtracting the value of the systemic heliocentric velocity $V_{\odot}$ without correcting for the galaxy inclination.

4.2. Stellar kinematics

The major-axis stellar kinematics is measured out to about $30''$ on each side of the nucleus (Fig. 5). The velocity curve is characterized by a central plateau showing no rotation for $|r| \lesssim 3''$. At larger radii we observe an asymmetrical increasing of the rotation velocity on both sides of the major axis. The rotation velocity at the farthest measured point is about 90 km s^{-1} and about 200 km s^{-1} on the receding and approaching side, respectively. The velocity dispersion profile displays a central dip of about 60 km s^{-1}. In fact the velocity dispersion is 150 ± 20 km s^{-1} at $r \simeq 0''$ and about 210 km s^{-1} at $|r| \simeq 1''.5$. Outwards it decreases reaching an almost constant value of 100 km s^{-1} for $|r| > 6''$.

The minor-axis stellar kinematics extends to $-6''$ on the NW side and to $+9''$ on the SE side, respectively (Fig. 6). The velocity curve shows a steep gradient in the nucleus ($|r| \lesssim 3''$) rising to maximum rotation of about 85 km s^{-1} ($\Delta V_{\star} = 170 \pm 18$ km s^{-1}). At larger radii it tends to drop to a zero value on the SE side, while it remains almost constant at about 40 km s^{-1} on the NW side. Along the minor axis the stellar velocity dispersion profile has a more uncertain behaviour. It seems to fall from a central value of 154 ± 15 km s^{-1} to about 80 km s^{-1} further out.

4.3. Ionized-gas kinematics

The major-axis ionized gas kinematics is measured to about $60''$ from the center on both sides of the galaxy (Fig. 5). The gas velocity curve is radially asymmetric. On the SW side it exhibits a sharp gradient reaching about 110 km s^{-1} at $-7''$. Further out it shows bumps and wiggles and the velocity oscillates between 93 ± 3 km s^{-1} and 111 ± 3 km s^{-1} in the radial range between $-7''$ and $-33''$. Then it rises to about 170 km s^{-1} at $-57''$. Along the NE side the rotation velocity increases almost linearly with radius from 0 km s^{-1} to about 170 km s^{-1} between $0''$ and $+25''$, then it remains approximately constant up to $+35''$. Outside it declines to about 140 km s^{-1} at $+61''$. The gas velocity dispersion is lower than 70 km s^{-1} at all radii.

Along the minor axis the measurements extend between $-6''$ and $+2''$ (Fig. 6). No rotation is detected and the corresponding velocity dispersion declines from about 60 km s^{-1} to 0 km s^{-1} moving outwards from the center.

The fact that the same velocity dispersion corresponds to different rotation velocities on both sides of the galaxy along its major axis, shows that the ionized gas is an unreliable tracer of the circular rotation in the observed radial range of NGC 4672. Besides, this kind of disturbed rotation curves are common in disk galaxies, as shown in a recent study of the optical velocity curves of a large number of Virgo S0's and spirals by Rubin et al. (1999).

The analysis of the interplay between the ionized gas and stellar kinematics along both the major and minor axis shows a decoupling between the rotation of the gas and that of the inner ($|r| < 5''$) stellar component. Similarly, the stellar velocity curves indicate that a kinematical decoupling between the inner and outer stellar components is also present as well.

5. Discussion and conclusions

In the previous sections we have pointed out that NGC 4672 is an early-type disk galaxy (most probably an Sa spiral) with a prominent bulge sticking out from the plane of the disk rather than a polar-ring S0 galaxy. In addition to this remarkable orthogonal geometrical decoupling between bulge and disk, the stellar velocity field of NGC 4672 is characterized by a central zero-velocity plateau along the galaxy major axis and by a steep velocity gradient along the minor axis. This means that in the inner regions of the bulge we are in the presence of a stellar core, which is rotating perpendicularly to the disk. We conclude that NGC 4672 has the same morphological (*i.e.*, a bulge elongated perpendicularly to the disk) and kinematical (*i.e.*, a stellar velocity gradient along the bulge major axis) properties as those observed recently by Bertola et al. (1999) in the Sa spiral NGC 4698.

As pointed out by Bertola & Corsini (2000), the stellar rotation curve measured along the bulge major axis (corresponding to the disk minor axis) and the bulge minor axis of NGC 4672 and NGC 4698 both show the same radial trends (characterized by an inner velocity gradient and a zero-velocity plateau) which have been observed in the polar-ring elliptical AM 2020-504 along its major axis (corresponding to the ring minor axis) and minor axis, respectively.

AM 2020-504 is considered the prototype of ellipticals with a polar ring. It is constituted by two distinct structures: a mostly gaseous ring and a spheroidal E4 stellar component with their major axes perpendicular each other. It has been extensively studied by Whitmore et al. (1987, 1990), who first revealed the presence of a velocity gradient along the major axis of the spheroidal component, and by Arnaboldi et al. (1993a,b), who showed that the inner velocity gradient of the stars is followed at larger radii by a velocity decline to an almost constant zero value. Recent observations presented in Bertola & Corsini (2000) are consistent with these findings but also reveal that along the ring major axis the stars exhibit a zero-velocity plateau followed by a rising velocity curve, as in the cases of NGC 4698 and NGC 4672. Moreover no rotation of the ionized gas is observed along the spheroid major axis, contrary to the prediction of the warped model for the gaseous component by Arnaboldi et al. (1993a).

In spite of their morphological differences the early-type disk galaxy NGC 4672, the Sa spiral NGC 4698 and the polar-ring elliptical AM 2020-504 share two common characteristics:

(i) The major axis of the disk (or ring) component forms an angle of 90° with the major axis of the bulge (or elliptical) component, at least at a visual inspection. This orthogonal geometrical decoupling is uncommon among spiral galaxies (Bertola et al. 1991).

(ii) The stellar kinematics is characterized by a central zero-velocity plateau followed by a rising velocity curve along the disk (or ring) major axis, and by a steep velocity gradient followed by an almost zero constant velocity along the disk (or ring) minor axis. This indicates the presence of a kinematically isolated core, which is rotating perpendicularly with respect to the disk (or ring) component.

At this point we ask ourselves whether these galaxies also share similar formation processes. For NGC 4698 Bertola et al. (1999) suggested two alternative scenarios to explain the geometrical and kinematical orthogonal decoupling between the inner region of the bulge and the disk depending on the adopted (parametric or non-parametric) photometric decomposition.

If the parametric decomposition is adopted for NGC 4698, its surface-brightness distribution is assumed to be the sum of an $r^{1/4}$ bulge and an exponential thin disk. In this case the entire bulge structure is found to be elongated perpendicularly to the major axis of the disk. The fact that the velocity field of the bulge is characterized by zero velocity along the disk major axis and by a velocity gradient along the disk minor axis suggests that the intrinsic angular momenta of bulge and disk are perpendicular. This orthogonal decoupling of bulge and disk in NGC 4698 has been interpreted as the result of the formation of the disk component at a later stage, due to the acquisition of material by a triaxial pre-existing spheroid on the principal plane perpendicular to its major axis. For NGC 4698, according to the results of the photometric decomposition the peculiar velocity curve observed along the minor axis is representative of the rotation of its bulge. This is also true for NGC 4672, since the bulge contribution dominates the galaxy light along the minor axis in the region where we measured the stellar kinematics. However such a kind of rotation curve (which is quickly rising to a maximum value and then fall to about zero) is unrealistic for bulges, which are generally believed to be isotropic rotators (e.g., Kormendy & Illingworth 1982; Jarvis & Freeman 1985a,b).

If, on the other hand, the non-parametric photometric decomposition is adopted for NGC 4698, the surface-brightness distributions of bulge and disk do not depend on *a priori* fitting laws but are assumed to have elliptical isophotes of constant flattening. In this case the bulge of NGC 4698 should be round with only the inner portion elongated perpendicularly with respect to the disk major axis. For this reason the presence of an orthogonal decoupled core has been invoked by Bertola et al. (1999) to explain the observed photometric and kinematic

properties. This stellar core should be photometrically decoupled from the disk and kinematically decoupled with respect to both bulge and disk. With this in mind, it should be noticed that also the velocity fields of NGC 4672 and AM 2020-504 show the same discontinuity between the rotation of the inner and the outer regions as observed in NGC 4698. In elliptical galaxies such a discontinuity in the velocity field is the signature of the presence of a kinematically-decoupled core. Several formation scenarios have been proposed to explain the origin of isolated cores, but the decoupling between the angular momentum of a core and that of the host galaxy is generally interpreted as the result of a second event (see Bertola & Corsini 1999 for a review).

In NGC 4672 and AM 2020-504 the orthogonal geometrical decoupling between bulge and the disk (or ring) components is directly visible due to the high inclination of these galaxies. This geometrical decoupling implies that such objects did not form in a single event, as in the case of polar ring galaxies which are believed to be the result of an accretion event (Steiman-Cameron & Durisen 1982; Schweizer et al. 1983; Sparke 1986) or a merger (Bekki 1998). However it is hard to imagine that in NGC 4672 and AM 2020-504 the orthogonal disk component and the isolated core are the result of *two* distinct and unrelated accretion phenomena which occurred in different epochs.

Arnaboldi et al. (1993a,b) proposed a mechanism for the joint formation of both the kinematically-decoupled core and the polar ring of AM 2020-504. Following Sparke (1986), they considered the acquisition at a given angle of a large amount of external material by an oblate elliptical galaxy. Self-gravity acts on the gaseous disk, which is initially forming at constant inclination, to transfer angular momentum about the galactic pole from the outer material to that inside. In this way the outer gas moves towards nearly polar orbits forming the observed polar ring, while the inner gas is pushed away from the pole settling onto the equatorial plane of the host galaxy, and subsequently turning into the stars, which now constitute the isolated core. It is interesting to observe that for $|r| > 12''$ the kinematics of AM 2020-504 shows a non-rotating stellar body even if the galaxy has been classified as an E4 elliptical and modeled as an oblate spheroid (Arnaboldi et al. 1993a). Anyway there are a number of boxy E4 galaxies which show, slow or even no rotation of the stellar body, like NGC 1600 (Bender et al. 1994), NGC 5322 (Scorza & Bender 1995), and NGC 5576 (Bender et al. 1994). In particular, the case of NGC 1600 has been discussed recently by Matthias & Gerhard (1999), who concluded that the kinematics of the inner parts is consistent with a mostly radially anisotropic, axisymmetric three-integral distribution function.

This scenario has the attractive property that it explains both the orthogonal geometrical and kinematical decoupling between the spheroid and the ring components, as well as the kinematical isolation of the core observed in AM 2020-504, as the byproduct of an unique second event (represented by the skewed accretion of large amount of external material around an oblate spheroid) and its following dynamical evolution. Bertola & Corsini (2000) suggested that the same acquisition mechanism produced also the kinematically-decoupled cores in the center of the two disk galaxies NGC 4698 and NGC 4672. Therefore NGC 4672 and NGC 4698 are interpreted as the result of the disk accretion in a polar plane of a pre-existing oblate spheroid. Neither a velocity gradient along the disk minor axis nor a geometrical decoupling are expected if the acquisition process produces a disk settled on the equatorial plane of the spheroidal component.

The ionized-gas component displays a different behavior in the inner regions of NGC 4698 with respect to NGC 4672 and AM 2020-504. In NGC 4698 the gas rotation closely matches that of the stars (see Fig. 2 in Bertola & Corsini 2000). The observed kinematics suggests that in the center of NGC 4698 we are facing the ionized gas associated with the kinematically decoupled stellar component giving rise to the velocity gradient measured along the disk minor axis. On the contrary, no significant gas rotation is detected along the disk minor axis of NGC 4672 (Fig. 6) and AM 2020-504 (see Fig. 2 in Bertola & Corsini 2000), indicating that the inner ionized gas resides in the galaxy disk and is not associated with the isolated core. This can be explained if in NGC 4672 and AM 2020-504 the ionized gas settled onto the symmetry plane of the galaxy entirely transformed into stars leaving behind a nearly edge-on gas-depleted region, while in NGC 4698 this transformation is still in progress.

To identify candidates that may show the same features as NGC 4672 and NGC 4698 one should look for disk galaxies with an almost round bulge, whose isophotes appear to be elongated perpendicularly to the galaxy major axis after the subtraction of the disk surface brightness. To a first visual inspection of the photographic plates reproduced on the Carnegie Atlas of Galaxies (Sandage & Bedke 1994) the cases of NGC 2911 ($S0_3$(2) or S0 pec, Plate 49), NGC 2968 (amorphous or $S0_3$ pec, Plate 49), NGC 4448 (Sa (late), Plate 69) and NGC 4933 ($S0_3$ pec (tides), Plate 49) appear worthy of further investigation.

Multi-band photometry could reveal color differences between the stellar populations of the spheroid and possibly of the isolated core (as done by Carollo et al. 1997a,b for kinematically decoupled cores in ellipticals), allowing an estimate of their relative age if combined with high-resolution spectroscopy. Moreover, the latter will give us a detailed overview of the kinematics in the center of these galaxies and the analysis of the line profiles could unveil the dynamical nature of these cores (e.g., the case of the isolated core in the gE galaxy NGC 4365 studied by Surma & Bender 1995).

Several mechanisms have been proposed for bulge formation (see Wyse et al. 1997 for a review) in which the bulge formed before (e.g. by hierarchical clustering merging), at the same time (e.g. in a monolithic collapse) or after the disk (*e.g.* as a results of a secular evolution of the disk structure). Furthermore, there is evidence that disks and bulges can experience accretion events via infall of external material or satellite galaxies (see Barnes & Hernquist 1992 for a review of the different processes). Up to now none of these pictures is able to reproduce all the observed properties of disk galaxies along the Hubble sequence, leading to the idea that several of the mechanisms outlined in these different scenarios could have played a role in forming a galaxy (Bouwens et al. 1999).

The early-type disk galaxies NGC 4672 and NGC 4698 represent striking examples of galaxies which drastically changed morphology during their history and for which we suggest an inside-out formation process with the disk component accreted around a previously formed spheroid, according to the hierarchical clustering merging paradigm (Baugh et al. 1996; Kauffman 1996).

Acknowledgements. We thank Magda Arnaboldi and Linda Sparke for the useful discussion about the case of AM 2020-504. We are indebted to Bradley Whitmore for kindly proving us the image of NGC 4672 we used in Fig. 1. Marc Sarzi acknowledges the Max-Planck-Institut für Astronomie in Heidelberg for the hospitality while this paper was in progress. This research has made use of the Lyon-Meudon Extragalactic Database (LEDA) and of the NASA/IPAC Extragalactic Database (NED).

References

Aaronson M., Bothum G.D., Cornell M.E., et al., 1989, ApJ 338, 654
Arnaboldi M., Capaccioli M., Capellaro E., Held V.E., Sparke L., 1993a, A&A 267, 21
Arnaboldi M., Capaccioli M., Barbaro G., Buson L.M., Longo G., 1993b, A&A 268, 103
Arnaboldi M., Oosterloo T., Combes F., Freeeman K.C., Koribalsky B., 1997, AJ 113, 585
Arp H.C., Madore B.F., 1987, A Catalogue of Southern Peculiar Galaxies and Associations. Cambridge University Press, Cambridge
Barnes J.E., Hernquist L., 1992, ARA&A 30, 705
Baugh C.M., Cole S., Frenk C.S., 1996, MNRAS 283, 1361
Bekki K., 1998, ApJ 499, 635
Bender R., 1990, A&A 229, 441
Bender R., Saglia R.P., Gerhard O.E., 1994, MNRAS 269, 785
Bertola F., 1987, In: de Zeeuw T. (ed.) Structure and Dynamics of Elliptical Galaxies. IAU Symp. 127, Reidel, Dordrecht, p. 135
Bertola F., Corsini E.M., 1999, In: Barnes J., Sanders D.B. (eds.) Galaxy Interactions at Low and High Redshift. IAU Symp. 186, Kluwer Academic Press, Dordrecht, p. 149
Bertola F., Corsini E.M., 2000, In: Combes F., Mamon G.A., Charmandaris V. (eds.) Galaxy Dynamics: from the Early Universe to the Present. ASP Conf. Series 197, ASP, San Francisco, p. 115
Bertola F., Vietri M., Zeilinger W.W., 1991, ApJ 374, L13
Bertola F., Cinzano P., Corsini E.M., et al., 1996, ApJ 458, L67
Bertola F., Corsini E.M., Vega Beltrán J.C., et al., 1999, ApJ 519, L17
Bouwens R., Cayón L., Silk J., 1999, ApJ 516, 77
Bregman J.N., Hogg D.E., Roberts M.S., 1992, ApJ 387, 484
Carollo C.M., Franx M., Illingworth G.D., Forbes D.A., 1997a, ApJ 481, 710
Carollo C.M., Danziger I.J., Rich R.M., Chen X., 1997b, ApJ 491, 545
Corsini E.M., Pizzella A., Sarzi M., et al., 1999, A&A 342, 671
Corwin H.G., de Vaucouleurs A., de Vaucouleurs G., 1985, Southern Galaxy Catalogue. University of Texas, Austin (SGC)
Dawe J.A., Dickens R.J., Peterson B.A., 1977, MNRAS 178, 675
de Grijs R., 1998, MNRAS 299, 595
de Vaucouleurs G., de Vaucouleurs A., Corwin H.G.Jr., et al., 1991, Third Reference Catalogue of Bright Galaxies. Springer-Verlag, New York (RC3)
Dickens R.J., Currie M.J., Lucey J.R., 1986, MNRAS 220, 679
Garcia A.M., 1993, A&AS 100, 47
Guthrie B.N.G., 1992, A&AS 93, 255
Jarvis J.B., Freeman K.C., 1985a, ApJ 295, 314
Jarvis J.B., Freeman K.C., 1985b, ApJ 295, 324
Kauffman G., 1996, MNRAS 281, 487
Kent S.M., 1985, ApJS 59, 115
Kormendy J., Illingworth G., 1982, ApJ 256, 460
Lauberts A., Valentijn E.A., 1989, The Surface Photometry Catalogue of the ESO-Uppsala Galaxies. ESO, Garching bei München
Matthias M., Gerhard O., 1999, MNRAS 310, 879
Moshir M., Kopan G., Conrow T., et al., 1990, Infrared Astronomical Satellite Faint Source Catalogue, version 2.0
Reshetnikov V., Sotnikova N., 1997, A&A 325, 933
Richter O.-G., Sackett P.D., Sparke L.S., 1994, AJ 107, 99
Roberts M.S., Hogg D.E., Bregman J.N., et al., 1991, ApJS 75, 751
Rubin V.C., Waterman A.H., Kenney J.D., 1999, AJ 118, 236
Sackett P.D., Rix H.-W., Jarvis B.J., Freeman K.C., 1994, ApJ 436, 629
Sage L.J., Galletta G., 1993, ApJ 419, 544
Sandage A., Bedke J., 1994, The Carnegie Atlas of Galaxies. Carnegie Institution and Flintridge Foundation, Washington
Sandage A., Tammann G.A., 1981, A Revised Shapley-Ames Catalog of Bright Galaxies. Carnegie Institution, Washington
Schommer R.A., Bothun G.D., Williams T.B., Mould J.R., 1993, AJ 105, 97
Schweizer F., Whitmore B.C., Rubin V.C., 1983, AJ 88, 909
Scorza C., Bender R., 1995, A&A 293, 20
Simien F., de Vaucouleurs G., 1986, ApJ 302, 564
Sparke L.S., 1986, MNRAS 219, 657
Steiman-Cameron T.Y., Durisen R.H., 1982, ApJ 263, L51
Surma P., Bender R., 1995, A&A 298, 405
van Driel W., Combes F., Casoli F., et al., 1995, AJ 109, 942
Vega Beltran J.C., Corsini E.M., Pizzella A., Bertola F., 1997, A&A 324, 485
Whitmore B., McElroy D., Schweizer F., 1987, In: de Zeeuw T. (ed.) Structure and Dynamics of Elliptical Galaxies. IAU Symp. 127, Reidel, Dordrecht, p. 413
Whitmore B.C., Lucas R.A., McElroy D.B., et al., 1990, AJ 100, 1489
Wyse R.F.G., Gilmore G., Franx M., 1997, ARA&A 35, 637
Young J.S., Xie S., Kenney J.P.D., Rice W.L., 1989, ApJS 70, 699